

Analysis of the structure factor of dense krypton gas: Bridge contributions and many-body effects

G. C. Aers and M. W. C. Dharma-wardana

Division of Physics, National Research Council, Ottawa K1A 0R6, Canada

(Received 26 September 1983; revised manuscript received 11 January 1984)

The pair-correlation function $g(r)$ of the Kr-type model fluid with only pair interactions was calculated using the Rosenfeld-Ashcroft modification of the hypernetted-chain (HNC) equation which includes bridge diagrams, and gave results in excellent agreement with Monte Carlo $g(r)$ data. These bridge functions and the known pair potential were used to analyze the neutron-diffraction structure-factor data of Teitsma and Egelstaff, to determine the effective strength of the three-body potential as a function of the density assuming it to be of the Axilrod-Teller (AT) form. The strength of the effective three-body contribution $s = \nu/\nu_{\text{theor}}$, where ν_{theor} is the theoretical value, decreases for higher densities, suggesting that the many-body terms (beyond the Axilrod-Teller form) screen the AT interaction as the density increases. The results are very sensitive to the uncertainties in the structure factor $S(k)$ for small k if parameter optimization is used to determine the effective pair potential. However, prediction of the compressibility using $s=1$ allows us to conclude that ν_{theor} is consistent with the experimental data for low densities, to within the uncertainties in the presently available pair potentials and in the structure-factor data.

I. INTRODUCTION

The study of rare-gas fluids¹ has proved to be very useful both as a testing ground for theories of the fluid state and in the theory of interatomic potentials. Many properties of dilute gases (e.g., virial-coefficient data, viscosity, thermal conductivity and diffusion, spectroscopic and scattering data) have been used in extracting a pair potential^{2,3} which may be accepted with a high degree of confidence. However, attempts to use the structure factor $S(k)$ for the determination of interatomic potentials^{4,5} have been much less successful and open to considerable doubt.⁶ This is partly due to the approximate nature of the usual theories of liquids based on the hypernetted-chain (HNC) and Percus-Yevick (PY) type integral equations. Another practical difficulty arises from the fact that $S(k)$ values are experimentally available only for a limited window of k values, while the integral-equations formalism relies heavily on sensitive Fourier transformation techniques which require a full range of r or k values. The lack of a reliable integral equation can be overcome by resorting to machine simulation methods, as has been done in the recent study of the structure factor of Kr by Egelstaff and collaborators.^{7,8} However, their methods still require the extension of the data before Fourier techniques could be used.

The objective of the present paper is to use the Rosenfeld-Ashcroft modification⁹ of the HNC equation, viz., modified hypernetted chain (MHNC), to analyze the experimental structure factor of Kr. The simple HNC equation¹⁰ provides the pair-correlation function $g(r)$ of a fluid with pair interactions $U(r)$, under the assumption that the so-called bridge-diagram contributions $B(r)$ are zero. The Rosenfeld-Ashcroft modification may be looked upon as a procedure for substituting the true $B(r)$ by an equivalent hard sphere $B(r)$ using a self-consistently determined hard-sphere interaction. The di-

mensionless hard-sphere parameter η is self-consistently determined by choosing the value which best satisfies the compressibility sum rule. Thus the MHNC provides a simple, accurate theory of the fluid state and, unlike machine-simulation methods, yields $g(r)$, $S(k)$, and $c(k)$ for the full range of values of r and k . The method has already been used by the present authors¹¹ in a detailed analysis of the experimental structure factor of liquid Al. Both the experimental and theoretical problems are presumed to be simpler in the case of a rare-gas fluid. Since the pair potential for Kr is known with a high degree of confidence, the present study can be directed to the determination of the effective three-body potential which is consistent with the experimental structure factor, $[S(k)]_{\text{expt}}$.

The present study also demonstrates that, although it is true that the qualitative form of the structure factor is insensitive to the form of the potential, any attempts to get detailed agreement with the $[S(k)]_{\text{expt}}$ while at the same time demanding thermodynamic consistency, etc., requires that the detailed form of the potential should be correct. For example, the $S(k)$ of the pair fluid calculated from the Aziz² potential is slightly but distinguishably different from that of the pair potential of Barker *et al.*³

In Sec. II we discuss the model *Kr-pair fluid* with only pair interactions, and determine the parametrization of the bridge contributions. In Sec. III we discuss the inclusion of the three-body term in the MHNC equation. Finally, in Sec. IV we analyze the experimental data for $S(k)$ for Kr and determine the effective strength of the three-body potential as a function of the density.

II. BRIDGE CORRECTIONS IN THE Kr-PAIR FLUID

In this section we shall use the Kr-Kr pair potentials (Fig. 1) of Aziz,² viz., $U_{\text{Aziz}}(r)$ and that of Barker, Watts,

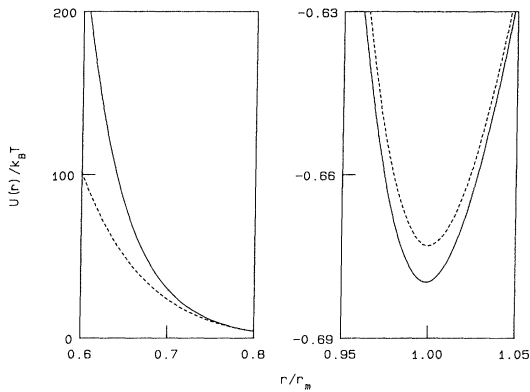


FIG. 1. Comparison of the Aziz (dashed curve) and the BWLSL (solid curve) pair potentials for Kr, in units of $r_m = 7.5715687$ a.u. Note that the Aziz potential is softer for small r and shallower at the minimum, with the minimum at $r/r_m = 1.001323$.

Lee, Schafer, and Lee³ (BWLSL), viz., $U_{\text{BWLSL}}(r)$, within the modified HNC scheme of Rosenfeld and Ashcroft,⁹ to generate the Kr-pair fluid structure factor $S(k)$. This also determines the bridge contribution $B(r)$ in terms of the hard-sphere parameter η , as a function of the density ρ . We shall show that the MHNC recovers the Monte Carlo results to well within the uncertainties of the simulation data. We also demonstrate that the direct use of the HNC equation to invert $S(k)$ does not yield the initial pair potential.

The failure of the HNC and similar equations is a consequence of the approximations inherent in them. The diagrammatic analysis of the pair-distribution function $g(r)$ leads to the form

$$g(r) = \exp[-\beta U(r) + N(r) + B(r)], \quad \beta = 1/k_B T, \quad (2.1)$$

where $N(r)$ and $B(r)$ are the so-called nodal and bridge-diagram contributions. The HNC approximation consists of neglecting the bridge terms. Then the Ornstein-Zernike equation can be coupled with (2.1) to give the set of closed equations:

$$g(r) = \exp[-\beta U(r) + N(r)], \quad (2.2)$$

$$N(r) = h(r) - c(r),$$

$$h(r) = g(r) - 1,$$

$$c(\vec{r}) = h(\vec{r}) - \rho \int h(|\vec{r} - \vec{r}'|) c(\vec{r}') d\vec{r}', \quad (2.3)$$

$$S(k) = 1 + \rho \int h(\vec{r}) e^{i\vec{k} \cdot \vec{r}} d\vec{r}. \quad (2.4)$$

The self-consistent solution of these equations for a given $U(r)$ constitutes the solution of the HNC equation to obtain an $S(k)$. On the other hand, given an $S(k)$, Eqs. (2.2)–(2.4) can be used to determine $U(k)$, thus defining the HNC-inversion procedure. Now, the solution of the HNC equation from a given $U(r)$ does not usually provide a good $S(k)$ or $g(r)$ which agrees with machine simulations. Hence it is not surprising that HNC inversion will not provide a good $U(r)$, unless there is reason to believe that the bridge terms are negligible.

For a given hard-sphere parameter η , the bridge contribution can be written⁹ in terms of the Percus-Yevick hard-sphere solution as

$$B_{\text{PY}}(r, \eta) = \begin{cases} -c_{\text{PY}}(r, \eta) - 1 - \ln[-c_{\text{PY}}(r, \eta)], & r < \sigma \\ g_{\text{PY}}(r, \eta) - 1 - \ln g_{\text{PY}}(r, \eta), & r > \sigma \end{cases} \quad (2.5a)$$

with

$$\eta = \pi \rho \sigma^3 / 6. \quad (2.5b)$$

Now η is chosen such that the compressibility determined from the $k \rightarrow 0$ limit of $S(k)$ agrees with that from the pressure. Thus, in the low-density or weak-coupling limit the MHNC reduces to the ordinary HNC equation with $\eta \rightarrow 0$. At higher densities, both the HNC and the PY equations fail to satisfy the compressibility sum rule, while the MHNC does so by the way it is formulated.

The values of η determined as a function of the density ρ from the BWLSL potential $U_{\text{BWLSL}}(r)$ and the Aziz potential $U_{\text{Aziz}}(r)$ are shown in Fig. 2. For later use, we have taken the same range of densities and the same temperature (297 K) as those used in Ref. 8 for $[S(k)]_{\text{expt}}$. The densities, to be denoted by $\bar{\rho}$, are expressed as the number of atoms per unit of reduced volume, $V_m = 4\pi r_m^3 / 3$, where r_m is arbitrarily chosen to be the minimum of the BWLSL pair potential ($r_m = 7.5715687$ a.u.). The value of η obtained is found to be linear in the range of densities studied and is well represented by

$$\eta = 0.0826\bar{\rho} \quad (2.6)$$

for both $U_{\text{Aziz}}(r)$ and $U_{\text{BWLSL}}(r)$.

Since Eq. (2.5b) becomes $\eta = \bar{\rho}(\sigma/2r_m)^3$ when written in reduced units, the linearity of Eq. (2.6) implies that the hard-sphere radius of σ/r_m is constant ($=0.871$) for this range of $\bar{\rho}$.

As can be seen from Fig. 2, the values of η were essentially the same for both BWLSL and Aziz potentials. However the $S(0)$ for the $U_{\text{Aziz}}(r)$ and $U_{\text{BWLSL}}(r)$ were slightly different, as will be shown later.

The hard-sphere radius σ defined by Eq. (2.5b) and

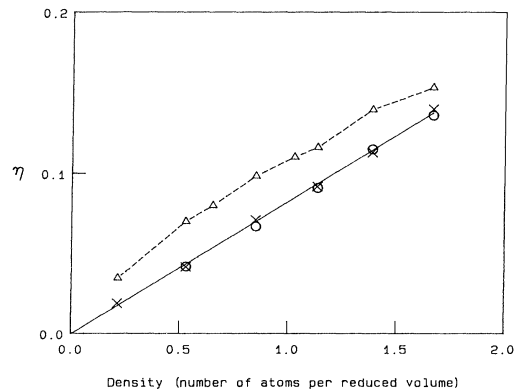


FIG. 2. Values of η obtained from the Rosenfeld-Ashcroft method for the BWLSL pair potential and the Aziz potential are shown as crosses and circles, respectively, together with the best linear fit (solid line). The triangles indicate the values of η which fit $[S(k)]_{\text{expt}}$ if the three-body term is neglected (dashed line is an aid to the eye).

modeled by Eq. (2.6) for the Kr fluid is a parametrization of the *bridge contributions* to the potential of mean force. This should be distinguished from the commonly used modeling procedure in which a structure factor generated from a hard-sphere potential is used to get a best fit to a given $S(k)$. The values of η (or σ) obtained by these different procedures are likely to be similar but not identical except for the hard-sphere fluid. Egelstaff *et al.*¹² use $\sigma/r_m = 0.88$ as a compromise best fit to two sets of experimental $S(k)$. This compares with $\sigma/r_m = 0.896$ and 0.839 if the hard-sphere criterion is chosen to be $U_{\text{BWLSL}}(r) = 0$ and $U_{\text{BWLSL}}(r) = (3/2)k_B T$, respectively. On the other hand, the hard-sphere radius σ/r_m obtained by the Rosenfeld-Ashcroft procedure for the bridge terms used here is about 0.87, for the range of densities studied here [see Eq. (2.6)]. Although σ is about the same in all these methods, the MHNC procedure used here reproduces $S(k)_{\text{expt}}$ to very high accuracy for the available range of k values, whereas simple fitting of a hard-sphere potential reproduces at best only the region about the first peak.

In Fig. 3 we show a typical comparison of the pair distribution $g(r)$ obtained using the MHNC procedure and the BWLSL potential with the Monte Carlo generated $g(r)$ at the same density, and from the same potential, due to Egelstaff, Teitsma, and Wang.⁷ Agreement with the machine-simulation (MS) results is excellent when MHNC is used; however, if the simple HNC equation is used ($\eta = 0$), the resulting $g(r)$ has a *higher peak* than that of the MS or MHNC generated $g(r)$.

In Fig. 4 we have shown (dashed line) the pair potential obtained by direct inversion, viz.,

$$\beta U(r) = N(r) - \ln[g(r)] \quad (2.7)$$

using the simple HNC (i.e., $\eta = 0$) equation. It is clear that the original potential (solid line) is not reproduced. It is accurately reproduced only when the bridge contributions are included. The inversion can also be done by fitting a parametrized form of the potential. Thus if the

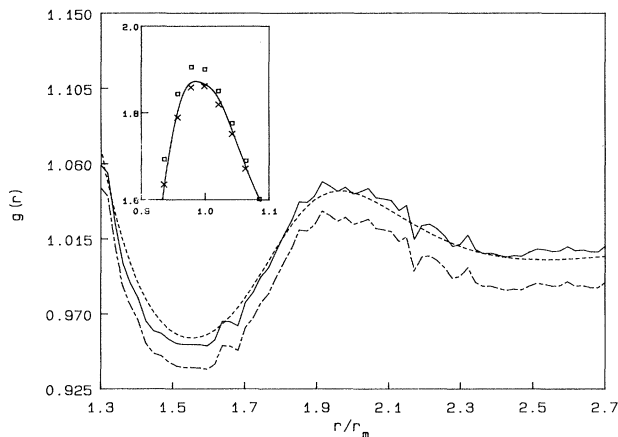


FIG. 3. Comparison of pair fluid $g(r)$ from MS and MHNC (both using the BWLSL potential) ($\eta = 0.133$) at $\bar{\rho} = 1.616$ atoms per reduced volume. The chained line is the raw MS data of Ref. 7; the solid line is the MS data corrected as in Ref. 7. The dashed line is the $g(r)$ from MHNC. The inset shows the first peak in $g(r)$: solid line—corrected MS data; crosses—MHNC; squares—simple HNC with $\eta = 0$.

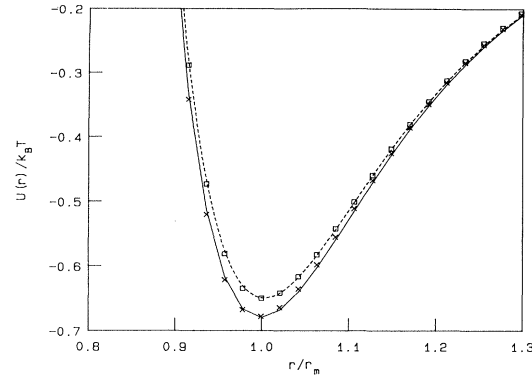


FIG. 4. Potentials obtained by inversion of the pair fluid $g(r)$ for Kr (see solid line in Fig. 3). Dashed line: result of direct HNC inversion as in Eq. (2.7); squares: HNC inversion with Aziz parametrization; crosses: MHNC inversion with Aziz parametrization; solid line: BWLSL pair potential.

same $g(r)$ is inverted with the Aziz parametrization of the pair potential, using the HNC and MHNC equations, the results obtained are shown as squares and crosses, respectively, in Fig. 4. This confirms the parametrization approach to inverting structure factors proposed in Ref. 11.

Having concluded that HNC (i.e., $\eta = 0$) or PY inversion is unreliable due to the lack of bridge terms, we also note that inversion of experimental data, $[S(k)]_{\text{expt}}$, is open to another source of error. The results are very sensitive to the manner in which the experimental data $[S(k)]_{\text{expt}}$, available in a limited range of k values, viz., $k_{\text{min}} \leq k \leq k_{\text{max}}$, are extended to small- k and large- k values. We have found that *this must be done self-consistently*, using the MHNC equation, and not just the HNC or PY equations, even at the lower densities of interest, if consistent results are to be obtained. An important conclusion from this discussion is that previous attempts to derive effective pair potentials, etc., by HNC or PY extension and inversion of structure-factor data could contain significant errors (see also Ref. 6).

III. THREE-BODY TERMS AND THE EFFECTIVE TWO-BODY POTENTIAL

In real Kr fluid the configurational energy E contains contributions beyond the pair potential. It is generally assumed that E can be written as

$$E = \sum_{i < 2} U(1,2) + \sum_{1 < 2 < 3} U_3(1,2,3) + \dots, \quad (3.1)$$

where the higher terms would depend on the coordinates of four, five, or more atoms. The triple or three-body potential $U_3(1,2,3)$ is the interaction energy of just three krypton atoms and can be analyzed¹³ into a number of terms

$$\begin{aligned} U_3(1,2,3) \rightarrow & v_{111}(1 + 3c_1c_2c_3)/r_1^3r_2^3r_3^3 \\ & + v_{112}f_{112}(c_1c_2c_3)/r_1^3r_2^4r_3^4 \\ & + v_{122}f_{122}(c_1c_2c_3)/r_1^4r_2^5r_3^5 \\ & + v_{222}f_{222}/r_1^5r_2^5r_3^5 + \dots, \end{aligned} \quad (3.2)$$

where v_{111} is the coefficient of the triple-dipole term and $c_1, c_2, c_3, r_1, r_2, r_3$ are the cosines and sides of the triangle formed by the three atoms. f_{112} , etc., are various functions of the angles. Of these contributions we assume, as usual, that the triple-dipole term (Axilrod-Teller potential) is the dominant contribution and write

$$U_3(r_1 r_2 r_3) = v(1 + 3c_1 c_2 c_3) / (r_1 r_2 r_3)^3 \quad (3.3)$$

for the three-body potential. If v is treated as a disposable parameter to be determined from experiment it will represent an "effective" three-body coefficient.

The inclusion of the three-body potential in the HNC or MHNC equation needs to be reviewed in view of the strong interplay between the bridge function $B(r)$, introduced using a hard-sphere repulsive interaction, and the effects of the three-body potential, which is *also repulsive* for our case. A diagrammatic analysis of the HNC equation in the presence of three-body potentials^{14,15} has been given by Rushbrooke and Silbert¹⁴ who show that the triplet potentials are *discarded* together with what we have called the bridge contributions, in constructing the HNC approximation. The leading elementary graphs which are discarded in HNC are shown in Fig. 5, where Fig. 5(a) has the standard structure with two-field points, while Fig. 5(b) contains a shaded triangle which arises from the irreducible three-body potential (see Ref. 14 for more details). In the pure pair fluid, diagrams like Fig. 5(a) are approximated by the Rosenfeld-Ashcroft procedure. When three-body terms are included, Fig. 5(a) and similar higher-order terms are still evaluated using the Rosenfeld-Ashcroft hard-sphere technique. However, Fig. 5(b) is treated as a contribution to the simple two-body potential to yield an effective potential $\tilde{U}(r)$. Thus, following Rushbrooke and Silbert,¹⁴

$$\tilde{U}(r) = U(r) - \rho\beta^{-1} \int e(1,3)f(1,2,3)e(2,3) d3, \quad (3.4)$$

where the coordinates of the third atom are integrated out. In (3.4)

$$f(1,2,3) = e(1,2,3) - 1 \approx v\beta(1 + 3c_1 c_2 c_3) / (r_1 r_2 r_3)^{-3}, \quad (3.5)$$

$$e(1,3) = \exp[-U(1,3)\beta]. \quad (3.6)$$

Because of the approximation in (3.5) the effective potential depends linearly on v . Such an approximation is justified when the triple potential is much weaker than $k_B T$. At 297 K, and for $r_1 = r_2 = r_3 = r_m$, where r_m is the minimum in the pair potential, the approximation is valid. But it fails for close-approach configurations which are in any case given a lower weight through the $e(1,3), e(2,3)$ factors. A partial resummation of diagrams can be used

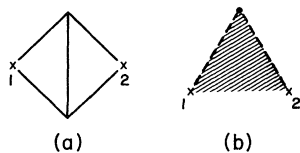


FIG. 5. The leading elementary graphs discarded in the simple HNC approximation. Dashed line: $e(1,2)$; solid line: $e(1,2) + 1$; shaded triangle: $f(1,2,3)$. See Eqs. (3.5) and (3.6).

to write a renormalized form of the effective potential

$$\tilde{W}(r) = U(r) - \rho\beta^{-1} \int g(1,3)f(1,2,3)g(2,3) d3. \quad (3.7)$$

However, for simplicity we have used the simpler form (3.4) together with the linearization approximation of (3.5). These simplifications are valid for $\bar{\rho} < 1$ and probably reasonable for all the densities studied here.

The inclusion of the three-body term to generate an effective pair potential does not change the relationship between the compressibility and the $k \rightarrow 0$ limit of $S(k)$. However, the compressibility derived directly from the pressure requires the evaluation of

$$P = \rho kT - \frac{\rho^2}{6} \int r(1,2)U'(1,2)g(1,2,\eta) d1 d2 - \frac{\rho^3}{18} \int \left[\frac{r_1 d}{d1} + \frac{r_2 d}{d2} + \frac{r_3 d}{d3} \right] \times U_3(1,2,3)g(1,2,3,\eta) d1 d2 d3 \quad (3.8)$$

and its density derivative.

In this expression $g(1,2,\eta)$ is the pair correlation function calculated using the effective potential (3.4) for a given bridge parameter η . We also need the triplet function $g(1,2,3,\eta)$. Hence, a determination of η by matching the two compressibilities, as was done for the pure pair potential, would be quite difficult. However, we note that when the BWLSL potential was replaced by the Aziz potential, the matching η was not affected (see Fig. 2). Since the difference between the BWLSL and Aziz potentials is of the same order as that between the pair potential and the effective pair potential, a new determination of η would seem to be superfluous. Thus the values of η determined from the pair fluid for each density (Fig. 2) were used in analyzing the experimental data.

IV. ANALYSIS OF THE EXPERIMENTAL STRUCTURE FACTOR OF Kr

The static structure factor of Kr in the density range of $0.1 < \bar{\rho} < 1.7$ atoms per unit volume (in reduced volume units), taken from Ref. 8, were used in the present study. The trial potential inclusive of the three-body term was taken as

$$\tilde{U}(1,2) = U(1,2) + s\rho \langle U_3 \rangle, \quad (4.1)$$

where

$$\langle U_3(r) \rangle = \int e^{-\beta U(1,3)} e^{-\beta U(2,3)} U_3(1,2,3) d3$$

and

$$U_3(1,2,3) = v_{\text{theor}}(1 + 3c_1 c_2 c_3) / (r_1 r_2 r_3)^3. \quad (4.2)$$

Also $U(1,2)$ is the pair potential of Barker *et al.* or of Aziz, as the case may be. $s = v/v_{\text{theor}}$ is the adjustable parameter representing the strength of the three-body term. v_{theor} is the theoretical coefficient of the three-body potential given as 2.288×10^{-82} erg cm⁹ in Ref. 13. The third atom averaged potential $\langle U_3(r) \rangle$ and the effective pair potential $\tilde{U}(1,2)$ with $s=1$ and $\bar{\rho}=1$ atom per unit re-

duced volume, for the BWLSL potential, are shown in Fig. 6.

The MHNC equation was now solved for each density with the corresponding bridge function, defined by the η at that density given by Eq. (2.6). The value of s was optimized to give the best fit to the experimental data. (The reader is referred to Ref. 11 for other details of the fitting procedure.) The experimental data are claimed to be accurate on the whole to better than 1%. The calculated structure factor $[S(k)]_{\text{calc}}$ reproduced the experimental data $[S(k)]_{\text{expt}}$ to high precision and was certainly within the error bars of $[S(k)]_{\text{expt}}$. The higher quality of the experimental data for Kr produced fits which are an order of magnitude better than those in Ref. 11. As discussed in Ref. 11, the inversion is sensitive to data for the small- k region and hence the percent change in s was also calculated with $[S(0)]_{\text{expt}}$ replaced by $[S(0)]_{\text{expt}} \pm 0.5\%$. The $S(0)$ obtained from the fit agreed with the input $[S(0)]_{\text{expt}}$ to five figures or better. The results obtained are given in Table I and displayed in Fig. 7. The uncertainty of 0.5% in $[S(0)]_{\text{expt}}$ was chosen for convenience although the compressibility determined from pressure-volume data may be somewhat more accurate.

The effect of a slight (i.e., $\pm 0.5\%$) error in $S(0)$, displayed as "error bars" in Fig. 7, shows that the determination of $s = \nu/\nu_{\text{theor}}$ becomes very sensitive to the quality of the data at lower densities. The value of s for $\bar{\rho} = 1.338$ lies above the trend of the rest of the data. This density corresponds to 5.15×10^{27} atoms m^{-3} in terms of the units of Ref. 8. The $S(Q)$ data for this density given in Table I of Ref. 8 for $Q = 1.6$ was taken to be 1.1395 (rather than 1.395) to be consistent with the data at the two neighboring densities. Also, the quoted experimental value $[S(0)]_{\text{expt}}$ for this density is seen to be somewhat lower than the value predicted by the fit to the other data points for $[S(0)]_{\text{expt}}$ shown in Fig. 8. When this is taken into account the apparent anomaly in the value of s (see Fig. 7) for $\bar{\rho} = 1.338$ largely disappears.

In view of the extreme sensitivity of $s = \nu/\nu_{\text{theor}}$ determined by fitting to $S(k)$ for a given $[S(0)]_{\text{expt}}$, we decided to reverse the procedure by setting $s = 1$, i.e., $\nu = \nu_{\text{theor}}$,

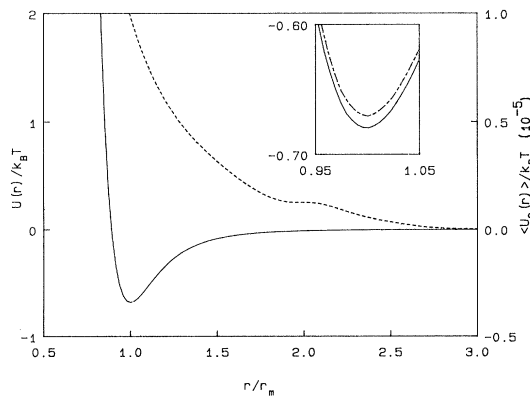


FIG. 6. Solid line: BWLSL pair potential; dashed line: third atom averaged three-body potential $\langle U_3(r) \rangle$. In the inset we show the BWLSL potential and the effective pair potential $\tilde{U}(r)$, Eq. (4.1) for $\bar{\rho} = 1$ atom per reduced volume, $s = 1$, and $T = 297$ K near r_m .

TABLE I. Analysis of experimental $[S(k)]_{\text{expt}}$ for Kr to determine the effective three-body strength parameter $s = \nu/\nu_{\text{theor}}$ where ν_{theor} is the theoretical value of 1618.64 a.u. s_{Aziz} and s_{BWLSL} are the values of s when the Aziz and the BWLSL potentials are used as the pair potential. Also shown with s_{BWLSL} is the uncertainty in s when $[S(0)]_{\text{expt}}$ is replaced by $[S(0)]_{\text{expt}} \pm 0.5\%$. The temperature is 297 K. The density $\bar{\rho}$ is the number of atoms per unit reduced volume $V_m = 4\pi r_m^3/3$, $r_m = 7.57157$ a.u. of BWLSL. Thus the density $\bar{\rho} = 1.668$ corresponds to 6.19×10^{27} atoms/ m^3 , used in Ref. 8.

$\bar{\rho}$	η	$S(0)$	$s_{\text{BWLSL}} = \nu/\nu_{\text{theor}}$	s_{Aziz}
1.668	0.1382	1.419	$0.5661 \pm 6\%$	0.8405
1.523	0.1262	1.490	0.7171	1.0280
1.388	0.1150	1.540	0.9658	1.3159
1.256	0.1041	1.594	$0.8652 \pm 6\%$	1.2599
1.136	0.0942	1.601	0.8829	1.3258
1.028	0.0852	1.582	0.9649	1.4595
0.8514	0.0706	1.526	$1.0461 \pm 11\%$	1.6518
0.6534	0.0542	1.425	1.1876	1.9846
0.5292	0.0439	1.348	1.2903	2.2783
0.4087	0.0339	1.269	$1.4380 \pm 42\%$	2.7197
0.2153	0.0178	1.140	$1.3159 \pm 200\%$	3.7516

and determining the compressibility ratio $S(0)$ which can then be compared with $[S(0)]_{\text{expt}}$. These results are shown in Table II. If we regard densities corresponding to $\bar{\rho} > 1$ as high densities, and $\bar{\rho} < 1$, i.e., less than one particle per sphere of radius r_m , as low densities, then it is clear that the theoretical three-body potential is in excellent agreement with $[S(0)]_{\text{expt}}$, especially for the BWLSL potential. The fluid from the Aziz potential inclusive of the theoretical three-body potential tends to be more compressible than the fluid from the BWLSL potential. This is also the case with the pure Aziz pair potential, as shown in Fig. 8. It may be conjectured that the higher compressibility of the Aziz pair fluid is a result of the softer inner wall of the Aziz potential. It should be noted that the inner wall of the Aziz potential has been fitted to

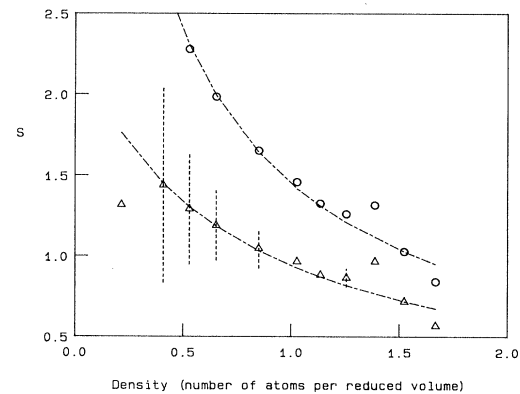


FIG. 7. Strength $s = \nu/\nu_{\text{theor}}$ of the three-body contribution as a function of $\bar{\rho}$. Triangles are the points obtained by fitting $[S(k)]_{\text{expt}}$ using MHNC and the BWLSL pair potential. The circles were for the Aziz potential. The ---- line is Eq. (4.4). The extremities of the vertical dashed lines are obtained with $[S(k=0)]_{\text{expt}} \pm 0.5\%$ used with the BWLSL potential (see Table I). Similar uncertainties (not shown) are found with the Aziz potential.

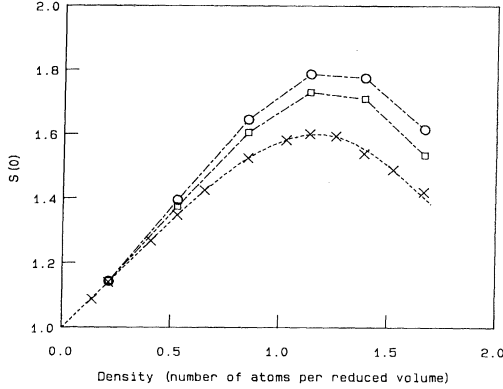


FIG. 8. Values of $S(k=0)$ for the Kr-pair fluid obtained from the MHNC are shown as squares and circles, respectively, for the BWLSL and Aziz potentials. The ---- lines are to guide the eye.) The values of experimental $[S(k=0)]_{\text{expt}}$ used in analyzing the experimental data are shown as crosses. The dashed line is a smoothed fit to $[S(k=0)]_{\text{expt}}$.

beam data, and also viscosity and thermal conductivity data up to 2000 K. This corresponds to nearly 10 times the well depth (0.01 a.u.) of the pair potential. This energy corresponds to $r/r_m \simeq 0.78$ and hence the inner wall for values of r/r_m smaller than, say, 0.8 may be felt to be less accurately known.

The strength parameter is expected to be relatively independent of the density if many-body effects [contributions beyond those of Fig. 5(b), etc.] are negligible. Since s is the only fitting parameter used, the effect of the n -body terms with $n > 3$ is to replace the three-body term by an effective three-body term

$$\tilde{W}_3 = U_3 + \rho \bar{U}_4 + \rho^2 \bar{U}_5 + \dots, \quad (4.3)$$

where $\rho \bar{U}_4$ is, for example, the four-body contribution averaged over the distribution of the fourth particle, and the terms similar to Fig. 5(b) but one order higher, together with the other three-body terms of Eq. (3.2) which were neglected. The series (4.3) might be approximately summed, using a geometrical Padé form:

TABLE II. Comparison of the compressibility ratios given by $S(k=0)$ with the experimental $[S(0)]_{\text{expt}}$ when the theoretical value ($\nu = \nu_{\text{theor}}$) of the three-body potential is used. $S(0)_{\text{BWLSL}}$, $S(0)_{\text{Aziz}}$ are from the BWLSL and Aziz potentials, respectively.

$\bar{\rho}$	$[S(0)]_{\text{expt}}$	$[S(0)]_{\text{BWLSL}}$	$[S(0)]_{\text{Aziz}}$
1.668	1.419	1.337	1.388
1.523	1.490	1.440	1.495
1.388	1.540	1.534	1.593
1.256	1.594	1.575	1.632
1.136	1.601	1.587	1.641
1.028	1.582	1.579	1.628
0.8514	1.526	1.529	1.568
0.6534	1.425	1.431	1.458
0.5292	1.348	1.354	1.374
0.4087	1.269	1.274	1.287
0.2153	1.140	1.141	1.147

$$\tilde{U}_3 = U_3 / [1 - \rho(\bar{U}_4/\bar{U}_3) + \rho^2(\bar{U}_5/\bar{U}_3) + \dots].$$

This suggests that we write the observed strength parameter s in the form

$$s = s^0 / (1 - \bar{\rho}t), \quad (4.4)$$

where s^0 and t are to be determined from the observed value of s .

The data of Table II strongly suggest that s^0 is unity. That is, at least for the low-density gas, the three-body term has the theoretical value, irrespective of whether the Aziz potential or the BWLSL potential were used for the pair effects. Also, the data of Tables I and II for $\bar{\rho} > 2$ show that a density-dependent screening of the strength parameter is in fact observed. If we discount the $\bar{\rho} < 1$ data in Table I but use the $\bar{\rho} > 1$ data as the latter is subject to smaller errors, the many-body screening parameter t in (4.4) is found to be approximately -0.2 for the BWLSL potential. The negative sign is in keeping with expectations and its magnitude implies that the higher-order terms are less important than the three-body potential. However, with the Aziz potential we see from Table I that the value of ν/ν_{theor} does not go below unity even at $\bar{\rho} = 1.5$ and hence the form (4.4) is not appropriate.

However, the data for higher densities is open to errors from the linearization approximation of Eq. (3.5), use of (3.4) rather than (3.7), as well as the use of η determined from the pair potential $U(r)$ rather than from a procedure involving Eq. (3.8) which contains the effect of $U_3(1,2,3)$. These approximations become increasingly invalid for $\bar{\rho} > 1$. Also, the Axilrod-Teller form is merely a convenient but not necessarily valid representation in lieu of the true three-body interaction valid at all r_1, r_2, r_3 , including small values of the arguments.

The experimental data, viz., $[S(k)]_{\text{expt}}$ can be fitted entirely using *only* the BWLSL pair potential $U_{\text{BWLSL}}(r)$ and a suitable hard-sphere parameter η which mimics *both* the bridge terms and the effect of the many-body terms. The corresponding values of η (for $s=0$ at all densities) are shown in Fig. 2. Although these η values reproduce $[S(k)]_{\text{expt}}$ very well, the compressibility sum rule is not satisfied.

Finally, we note that in Hoheisel's molecular dynamics study¹⁶ of the effect of the Axilrod-Teller (AT) potential on a Lennard-Jones liquid, he found that the apparent three-body contribution decreased with density, for the range of densities studied. This is in agreement with our results, but in Ref. 16 the many-body screening will arise merely from the higher-order iterations of two- and three-body clusters and will not involve terms corresponding to U_4 , U_5 , etc. Hoheisel does not give any quantitative results for the effective three-body term.

V. CONCLUSION

We conclude that the experimental structure data, viz. $[S(k)]_{\text{expt}}$, can be used within the Rosenfeld-Ashcroft modified hypernetted-chain equation to unravel the influence of many-body effects. These effects change the pair

potential to an effective pair potential, reducing the well depth by about a degree (1 K), lowering the compressibility, and contributing repulsively at all r . We have shown that the determination of parametrized potentials can be extremely sensitive to the compressibility $[S(0)]_{\text{expt}}$ used in the fitting process. When this uncertainty is taken into account the strength of the AT-type three-body potential obtained from $[S(k)]_{\text{expt}}$ is consistent with quantum theoretical estimates of the AT interaction parameter. The higher-order (many-body) terms provide an attractive

interaction which acts to screen the three-body contribution.

ACKNOWLEDGMENTS

We wish to thank Peter Egelstaff (Guelph University) for providing us with some tabulations of their⁷ Monte Carlo $g(r)$ for the Kr-pair fluid. We also wish to thank Mike Klein, National Research Council of Canada, for some useful discussions.

¹M. L. Klein and J. A. Venables, *Rare Gas Solids* (Academic, London, 1976), Vols. I and II.

²R. A. Aziz, *Mol. Phys.* **38**, 177 (1976).

³J. A. Barker, R. O. Watts, J. K. Lee, T. P. Schafer, and Y. T. Lee, *J. Chem. Phys.* **61**, 3081 (1974).

⁴P. G. Mikolaj and C. J. Pings, *J. Chem. Phys.* **46**, 1401 (1967); C. D. Andriess and E. Legrand, *Physica* **57**, 191 (1972).

⁵J. F. Karnicky, H. H. Reamer, and C. J. Pings, *J. Chem. Phys.* **64**, 4592 (1976).

⁶R. Taylor and R. O. Watts, *Solid State Commun.* **38**, 965 (1981).

⁷P. A. Egelstaff, A. Teitsma, and S. S. Wang, *Phys. Rev. A* **22**, 1702 (1980).

⁸A. Teitsma and P. A. Egelstaff, *Phys. Rev. A* **21**, 367 (1980).

⁹Y. Rosenfeld and N. W. Ashcroft, *Phys. Rev. A* **20**, 1208 (1976).

¹⁰R. Balescu, *Equilibrium and Nonequilibrium Statistical Mechanics* (Wiley, New York, 1975).

¹¹M. W. C. Dharma-wardana and G. C. Aers, *Phys. Rev. B* **28**, 1701 (1983); M. W. C. Dharma-wardana, F. Perrot, and G. C. Aers, *Phys. Rev. A* **28**, 344 (1983).

¹²P. A. Egelstaff, W. Glaser, D. Lichinsky, E. Schneider, and J. B. Suck, *Phys. Rev. A* **27**, 1106 (1983).

¹³R. J. Bell and I. J. Zucker, in Ref. 1, Vol. 1, Chap. 2, p. 148.

¹⁴G. S. Rushbrooke and M. Silbert, *Mol. Phys.* **12**, 505 (1967).

¹⁵G. Casanova, R. J. Dulla, D. A. Jonah, J. S. Rowlinson, and S. Saville, *Mol. Phys.* **18**, 589 (1970).

¹⁶C. Hoheisel, *Phys. Rev. A* **23**, 1998 (1981).